HHS Public Access

Author manuscript

Matrix Biol. Author manuscript; available in PMC 2017 September 01.

Published in final edited form as:

Matrix Biol. 2016 September ; 55: 63–76. doi:10.1016/j.matbio.2016.02.006.

Characterization of metabolic health in mouse models of fibrillin-1 perturbation

Tezin A. Walji[1], **Sarah E. Turecamo**[1], **Antea J. DeMarsilis**[1], **Lynn Y. Sakai**[2], **Robert P. Mecham**[1], and **Clarissa S. Craft**[1,*]

[1]Department of Cell Biology & Physiology, Washington University School of Medicine, St. Louis, MO, USA 63110

[2]Department of Biochemistry & Molecular Biology and Molecular & Medical Genetics, Oregon Health & Science University and Shriners Hospital for Children, Portland, OR, USA 97201

Abstract

Mutations in the microfibrillar protein fibrillin-1 or the absence of its binding partner microfibril-associated glycoprotein (MAGP1) lead to increased TGFβ signaling due to an inability to sequester latent or active forms of TGFβ, respectively. Mouse models of excess TGFβ signaling display increased adiposity and predisposition to type-2 diabetes. It is therefore interesting that individuals with Marfan syndrome, a disease in which fibrillin-1 mutation leads to aberrant TGFβ signaling, typically present with extreme fat hypoplasia. The goal of this project was to characterize multiple fibrillin-1 mutant mouse strains to understand how fibrillin-1 contributes to metabolic health. The results of this study demonstrate that fibrillin-1 contributes little to lipid storage and metabolic homeostasis, which is in contrast to the obesity and metabolic changes associated with MAGP1 deficiency. MAGP1 but not fibrillin-1 mutant mice had elevated TGFβ signaling in their adipose tissue, which is consistent with the difference in obesity phenotypes. However, fibrillin-1 mutant strains and MAGP1-deficient mice all exhibit increased bone length and reduced bone mineralization which are characteristic of Marfan syndrome. Our findings suggest Marfan-associated adipocyte hypoplasia is likely not due to microfibril-associated changes in adipose tissue, and provide evidence that MAGP1 may function independently of fibrillin in some tissues.

Keywords

fibrillin; MAGP; microfibril; diabetes; adipose tissue; TGFβ

[*]Address correspondence to: Clarissa S. Craft, Campus Box 8228, 660 S. Euclid Ave.; St. Louis, MO 63110. Phone: 314-362-2254. Fax: 314-362-2252. clarissa.craft@wustl.edu.

Competing financial interests: The authors declare no competing financial interests.

Introduction

Microfibrils are extracellular matrix (ECM) structures that contribute to tissue strength and provide instructional signals that affect cellular differentiation and function [4, 23, 31, 32]. These multi-protein filaments appear in early development and are found in almost all tissues [22, 25]. The core proteins are the fibrillins, which are encoded by three genes in humans (*FBN*-1, -2, and -3) but only two functional genes in mice (*Fbn*-1, -2) [4, 23, 32]. Mutations in fibrillin-1 give rise to the autosomal dominant disease Marfan syndrome (MFS), which is associated with musculoskeletal, ocular, pulmonary and cardiovascular anomalies [14, 21]. Relevant to this project, individuals with MFS also tend to have reduced fat and muscle mass.

Significant progress towards understanding the molecular pathogenesis of MFS was made with the discovery that the transforming growth factor-beta (TGFβ) signaling pathway was dysregulated in fibrillin-1 mutant mice and that antagonizing this pathway could prevent or reverse pulmonary and cardiovascular phenotypes [10, 18, 19]. These finding were translated clinically when elevated circulating TGFβ was demonstrated in individuals with MFS [9, 17]. Fibrillin-1 mediates TGFβ signaling by stabilizing the latent TGFβ complex in the ECM through direct interactions with the latent TGFβ binding proteins (LTBPs) [12, 16, 20]. Fibrillin-1 can also regulate TGFβ signaling indirectly through its binding partner MAGP1, which tethers the *active* form of TGFβ to the microfibril [28]. Consequently, loss of MAGP1 also causes activation of the TGFβ signaling pathway [5-7].

TGFβ has been demonstrated to influence energy expenditure and adipogenesis, and thereby whole body adiposity [15, 26, 27, 29, 30]. Serum TGFβ positively correlates with BMI, reducing TGFβ signaling results in leaner mice, and TGFβ blockade can protect mice against diet-induced obesity/diabetes. Increased circulating TGFβ in MFS would therefore be predicted to cause excess adiposity and predisposition to metabolic disease, not reduced adiposity. Thus, extreme leanness associated with MFS confounds our understanding of fibrillin-1's mechanism of action.

This project utilized three mouse models of fibrillin-1 disruption to address fibrillin-1's contribution to adipose tissue homeostasis. The first, fibrillin-1 gene inactivation ($Fbn1^{-/-}$), provided a model of fibrillin1 -loss of function. Because mice homozygous for the mutation die shortly after birth, we used $Fbn1^{+/-}$ animals as a model of fibrillin-1 haploinsufficiency. In the second model, a missense mutation of fibrillin-1 (C1039G) disrupts microfibril assembly and homozygosity of this mutation is also associated with early postnatal death [13]. Therefore, heterozygous mice ($Fbn1^{C1039G/+}$) were used as a model of dominant negative effect on microfibril organization and loss of function. The third model utilized mice homozygous for fibrillin-1 with exon 7 deleted ($Fbn1^{H1\Delta/H1\Delta}$). Exon 7 encodes the putative site that mediates interaction of fibrillin-1 with LTBPs [20]; these mice assemble microfibrils normally but should not be able to properly sequester the large latent TGFβ complex [3]. The metabolic health of mice associated with these three fibrillin-1 models was compared to mice deficient in MAGP1 ($Mfap2^{-/-}$). Loss of this microfibril-associated protein has no consequence on microfibril structure but does result in increased TGFβ signaling in adipose tissue, excess adiposity and metabolic disease [6, 28]. Therefore, MAGP1-deficient

mice (*Mfap2*$^{-/-}$) represent a reference phenotype for reduced metabolic health that is associated with dysregulated TGFβ signaling in the absence of microfibril structural changes (similar to the *Fbn1*$^{H1\Delta/H1\Delta}$ mouse).

Contrary to expectations based on the human Marfan phenotype, we found that none of the fibrillin-1 mutant mice displayed a lean phenotype; instead, by adulthood these mice tended to be slightly heavier and more insulin resistant than their wild-type littermates. However, these phenotypes are minor relative to the weight gain and metabolic dysfunction observed in the *Mfap2*$^{-/-}$ mice. Furthermore, we were able to detect elevated TGFβ signaling in *Mfap2*$^{-/-}$ adipose tissue but not in any of the fibrillin-1 mutant mice. MFS-associated skeletal anomalies have been documented in mouse models of fibrillin-1 disruption [24]. Despite lacking a metabolic phenotype, all three fibrillin-1 mutant lines recapitulated the Marfanoid features of long bone overgrowth and reduced bone mass. These anomalies were consistent with both elevated TGFβ signaling and the skeletal phenotypes of MAGP1-deficient mice. Together, our data suggest that fibrillin-1 and MAGP1 have similar TGFβ regulatory roles in the skeleton but diverge in terms of energy metabolism or lipid storage.

Results

Fibrillin-1 disruption has little effect on fat and lean mass in mice

Using echoMRI, we showed that alterations in microfibril assembly (*Fbn1*$^{C1039G/+}$), fibrillin-1 haploinsufficiency (*Fbn1*$^{+/-}$) or the absence of fibrillin-1's LTBP-binding domain (*Fbn1*$^{H1\Delta/H1\Delta}$) are associated with a modest increase (5-19%) in whole body fat mass by 6 months. Statistical significance was reached only in *Fbn1*$^{C1039G/+}$ mice (Figure 1a). Lean-muscle mass was slightly reduced in 6- and 8-week old *Fbn1*$^{C1039G/+}$ mice but this difference failed to reach statistical significance (Figure 1b). In contrast, *Fbn1*$^{H1\Delta/H1\Delta}$ mice had increased muscle mass at the same age (6-8 weeks) but this phenotype was lost by 24 weeks. Body weight changes correlated with alterations in fat and lean mass, with *Fbn1*$^{C1039G/+}$ mice weighing more than their littermate controls at 24 weeks due to increased fat mass while the *Fbn1*$^{H1\Delta/H1\Delta}$ mice were significantly heavier at 6 and 8 weeks due to the increase in lean mass (Figure 1c). As shown previously [6], loss of MAGP1 (*Mfap2*$^{-/-}$) resulted in significant fat and weight gain (220%), and an appreciable decrease in lean muscle mass (-8%); likely due to ectopic lipid accumulation.

Metabolic tissues including liver, brown adipose tissue (BAT), subcutaneous white adipose tissue (scWAT) and epididymal white adipose tissue (epWAT) were collected from 8 and 24 week old mice. Tissue wet weights are shown in Figure 2a-b. At 8 weeks, both *Fbn1*$^{C1039G/+}$ and *Fbn1H*$^{1\Delta/H1\Delta}$ mice had slightly enlarged livers and BAT. At 24 weeks, *Fbn1*$^{C1039G/+}$ mice showed a slight increase in scWAT, but lost the BAT and liver mass increase. *Fbn1*$^{+/-}$ mice, interestingly, show a statistically significant increase in white adipose tissue mass (scWAT and epWAT). *Fbn1H*$^{1\Delta/H1\Delta}$ mice retained the increase in liver mass, but also showed a trend in increased epWAT mass. H&E stained sections of epWAT tissue from these mice suggested that the increase in fat pad mass is from adipocyte hypertrophy (Figure 2c). However, the change in tissue sizes observed in fibrillin-1 mutant mice is relatively insignificant compared to the accumulation of fat observed in tissues from MAGP1-deficient mice.

These findings imply that neither reduced microfibril assembly by fibrillin-1 (*Fbn1*$^{C1039G/+}$, *Fbn1*$^{+/-}$) nor homozygous loss of fibrillin-1-LTBP binding (*Fbn1*$^{H1\Delta/H1\Delta}$) disrupts lipid accumulation in adipose depots. The extreme weight gain in *Mfap2*$^{-/-}$ mice introduces the possibility that MAGP1 could function independent of fibrillin-1.

Insulin sensitivity is slightly reduced in adult fibrillin-1 mutant mice

Insulin and glucose tolerance testing (ITT, GTT) were used to assess insulin sensitivity and glucose clearance. Both tests were performed in young and adult (6-,8-,24-weeks) fibrillin-1 mutant mice. Insulin sensitivity was normal at 6 and 8 weeks for *Fbn1*$^{C1039G/+}$ and *Fbn1*$^{+/-}$ mice. *Fbn1*$^{H1\Delta/H1\Delta}$ mice, however, had reduced insulin sensitivity at 6 weeks that resolved by 8 weeks (Figure 3a-b). By 24 weeks, insulin sensitivity was slightly, but significantly, reduced in all fibrillin-1 mutant mice (Figure 3c). In keeping with the appreciable differences between fibrillin-1 and MAGP1 mutant mice, Figure 3c demonstrates that by 24 weeks, *Mfap2*$^{-/-}$ mice are both hyperglycemic and insulin resistant. Glucose tolerance (clearance) is normal in all ages (6-,8-, 24-weeks) of fibrillin-1 mutant mice, which is in stark contrast to *Mfap2*$^{-/-}$ mice that have severely reduced glucose tolerance/clearance at 24 weeks (Figure 4).

Skeletal anomalies are common in fibrillin-1 and MAGP1 mutant mice

Despite differences in metabolic phenotypes, all fibrillin-1 and MAGP1 mutant mice have skeletal anomalies similar to those seen in individuals with Marfan syndrome (Figure 5). Classical features of Marfan syndrome include increased height, long bone overgrowth and reduced bone mass. In the mice, body length, measured from nose tip to tail base, was slightly increased in the fibrillin-1 mutant animals at 8 weeks (Figure 5a). By 24 weeks, increased body length was evident in all mutant mice relative to WT controls except for *Fbn1*$^{+/-}$ mice that did not reach statistical significance. It is important to note that 24-week body length measurements in fibrillin-1 mutant mice are undervalued due to spine curvature. Bone length was assessed by digital caliper measurement of tibias. All fibrillin-1 mutant mice had significant long bone overgrowth, detectable by 8-weeks and persistent through 24-weeks (Figure 5b).

Microcomputed tomography (μCT) demonstrated that all four mutant lines (fibrillin-1 and MAGP1) also display a statistically significant reduction in trabecular bone volume and mineralization by 24 weeks (Figure 6a). Three-dimensional reconstruction of the fibrillin-1 and MAGP1 mutant bones highlight the reduction in bone mass. Fibrillin-1 and MAGP1 mutant mice had little-to-no change in cortical bone volume and mineralization, which is not unexpected given the slow rate of cortical bone turnover (Figure 6b). Additional bone parameters gained by μCT are detailed in supplemental tables 1 and 2.

Skeletal anomalies in both *Fbn1*$^{H1\Delta/H1\Delta}$ and *Mfap2*$^{-/-}$ mice provides evidence that loss of microfibril-mediated regulation of TGFβ is sufficient to cause Marfanoid skeletal features as these mutant mice assemble normal fibrillin microfibrils but have reduced interaction with TGFβ. However, the bone phenotypes were most striking in the *Fbn1*$^{C1039G/+}$ mice suggesting improper microfibril assembly is also an additive factor.

Tissue specific regulation of TGFβ by fibrillin-1

Through interactions with the latent TGFβ binding protein (LTBP), the fibrillins are able to regulate the bioavailability of TGFβ by sequestering the TGFβ large latent complex into the ECM. MAGP1 also regulates the TGFβ signaling pathway but through direct binding to the "active" form of TGFβ. Our previously published studies show that MAGP1-deficient adipose tissue and bone have elevated TGFβ signaling [6]. To discern whether differences in TGFβ signaling accounted for the contrasting metabolic and bone phenotypes in the fibrillin-1 and MAGP1 mutant mice, we assessed TGFβ signaling in adipose tissue and bone through visualization of smad-2/3 activation (smad-2/3 phosphorylation). Epididymal fat and marrow-flushed tibia lysates were generated from fibrillin-1 mutant, MAGP1-deficient, and WT control animals. Immunoblots were performed using an antibody detecting receptor-activated smad-2/3 protein (Figure 7). We found fibrillin-1 perturbation had little consequence on smad-2/3 phosphorylation in mutant epWAT lysates, relative to WT controls. In contrast, smad phosphorylation was higher in MAGP1-deficient WAT lysate relative to both fibrillin-1 mutants and WT controls. Bone lysates revealed a modest increase in smad activation in both fibrillin-1 mutant and MAGP1-deficient mice. These findings indicate that fibrillin-1 perturbation alone is insufficient to elevate TGFβ bioavailability in adipose depots, and provides a biological explanation for the divergent metabolic phenotypes between MAGP1 and fibrillin-1 mutant mice.

Discussion

Microfibrils are complex multi-protein structures in which polymers of fibrillin proteins create a scaffold for auxiliary proteins to assemble upon. The deletion or mutation of microfibril proteins in mice has produced both overlapping and divergent cardiovascular, pulmonary and musculoskeletal phenotypes. Table 1 summarizes published phenotypes from several microfibril mutant mice. This manuscript adds the following information to the table: The fibrillin-1 mutations used in our study (*Fbn1*$^{+/-}$, *Fbn1*$^{H1\Delta/H1\Delta}$, or *Fbn1*$^{1039G/+}$) do not cause lipodystrophy. Instead, these mice have slightly increased adiposity and reduced insulin sensitivity by 6 months of age. These phenotypes, however, are insignificant relative to the worsened metabolic health of MAGP1-deficient (*Mfap2*$^{-/-}$) mice observed previously as well as in the current study using a new *Mfap2*$^{-/-}$ strain [6]. With respect to skeletal development, all mutant mice (fibrillin-1 and MAGP1) display increased body and tibia length as early as 8 weeks of age. Trabecular bone mass and mineral density were slightly reduced in fibrillin-1 mutant mice by 8 weeks of age, gaining statistical significance by 24 weeks. Cortical bone mass and mineral density were not significantly changed. Our findings are indicated in Table 1 by bolded/italicized text.

The original goal of this project was to assess whether disruption of fibrillin-1 microfibril assembly or fibrillin-1-LTBP binding (TGFβ sequestration) in mice would cause changes in lean and fat mass observed clinically in individuals with Marfan syndrome. An extension of this question was whether a change in body composition would result in impaired glucose metabolism that is often associated with lipodystrophy. None of the three fibrillin-1 mutant strains exhibited reduced fat or muscle mass relative to their littermate WT controls. Instead the fibrillin-1 mutant mice showed a slight increase in fat mass. Marfan syndrome is

associated with elevated TGFβ signaling [14, 21], and can help explain the trend toward weight gain and slight insulin resistance in the fibrillin-mutant mice as TGFβ supports adipogenesis and adipocyte hypertrophy by impairing energy expenditure [1, 11, 29]. However, the adiposity and glucose metabolism phenotypes in the fibrillin-1 mutant mice are minor compared to other models of enhanced TGFβ signaling, including MAGP1-deficient mice. Together, these findings suggest that fibrillin-1 mutation or loss is not sufficient to perturb TGFβ signaling in metabolic (adipose) tissues. This concept is supported by our finding that TGFβ signaling (measured by smad phosphorylation) is significantly elevated in adipose tissue from MAGP1-deficient mice but not fibrillin-1 mutant animals. We cannot rule out the possibility that fibrillin-2 is compensating for the loss of fibrillin-1, but we have previously shown that fibrillin-2 (*Fbn2*) expression in white adipose tissue is below the detection limits of RT-qPCR [6].

In contrast to metabolic changes, both fibrillin-1 and MAGP1 mutant mice display reduced trabecular bone mass and long bone overgrowth. These findings are important as they indicate that loss of either fibrillin-1 or MAGP1 is sufficient to perturb TGFβ signaling in bone and suggest fibrillin-1 and MAGP1 contribute equally or similarly to the regulation of bone turnover. The exaggerated skeletal phenotype in $Fbn1^{C1039G/+}$ mice likely highlights fibrillin-1's dual functions: TGFβ regulation and tissue organization. TGFβ activity is increased in all four mutant mouse models, but only $Fbn1^{C1039G/+}$ mice have perturbed microfibril assembly. We speculate that altered microfibril assembly has consequences for bone mechanoproperties and these changes are an additive factor to bone overgrowth and reduced bone mass.

The observation that MAGP1 loss elevates adipose tissue TGFβ signaling and causes metabolic disease, but not fibrillin-1 loss, also indicates that MAGP1 may function in a microfibril-independent manner. Adipose tissue extracellular matrix must remodel to accommodate excess lipid accumulation associated with diet-induced obesity. We previously reported that MAGP1 expression is differentially regulated in obese humans and mice fed a high-fat diet [6]. Unlike MAGP1, fibrillin-1 expression in adipose tissue is unchanged by metabolic challenge (diet-induced obesity). Further, MAGP1 has been shown to interact with collagen-VI, but not collagens-I, -III, -V [8]. Collagen-VI is differentially expressed in the adipose tissue of obese animals similar to MAGP1, and the absence of MAGP1 impairs obesity-induced expression of Col-VI (data not shown). The capacity of MAGP1 to function on alternative ECM structures is a topic of future studies.

In summary, our findings provide a thorough characterization of metabolism and bone remodeling in mouse models of Marfan syndrome. These studies clearly demonstrate that neither fibrillin-1 loss of function nor its ability to sequester TGFβ, in mice, is sufficient to mimic fat and muscle hypoplasia observed clinically. Further, our data support MAGP1 as a critical regulator of energy metabolism and provides evidence that MAGP1 might function in a fibrillin-1 independent manner.

Experimental Procedures

Animals and diets

All animals used in the study were males on the C57BL/6 background, housed in a pathogen-free animal facility, and were fed standard chow ad libitum. The fibrillin-1 C1096G mouse was purchased from Jackson Laboratories, the fibrillin-1 H1Δ mouse was a gift from Dr. Lynn Sakai [3] (Oregon Health Science University), and the fibrillin-1 *Fbn1*$^{+/-}$ (MgN) mouse was a gift from Dr. Francesco Ramirez [2] (Mount Sinai School of Medicine). The MAGP1-deficient (*Mfap2*$^{-/-}$) mouse line was newly generated using ES cells purchased from KOMP Repository (Davis, CA). The KOMP targeted, C57BL/6-derived ES cells (Mfap2$^{tm1a(KOMP)Wtsi}$) were injected into blastocysts from C57BL/6 donors and transferred into pseudopregnant C57BL/6 females. Offspring were maintained on the C57 background and are a different line than those used in previous studies [5, 7, 28].

Body composition, glucose and insulin tolerance testing

Body mass composition (lean and fat mass) was quantified using the EchoMRI 3-in-1 model instrument (Echo Medical Systems, Houston, TX). For glucose tolerance tests (GTTs), mice were fasted 6 hours before a 1g/kg dextrose injection. For insulin tolerance tests (ITTs), mice were fasted 6 hours prior to a 0.75 unit/kg Humulin-R insulin injection (Lilly, Indianapolis, IN). Dextrose and insulin were delivered by intraperitoneal injection. Tail blood glucose concentration was measured at the indicated intervals using Contour strips and meter (Bayer, Whippany, NJ).

Tissue collection

Tissue was collected at 8 and 24 weeks. Mouse fur was sprayed with 70% EtOH, then interscapular brown adipose tissue (BAT), subcutaneous inguinal white adipose tissues (scWAT), epididymal white adipose tissue (epWAT), and liver lobes were collected. Tissues were cleaned thoroughly of all contaminates (hair, connective tissue etc) then frozen or formalin fixed.

Histology

Tissues were fixed in 10% buffered formalin, dehydrated by an ethanol gradient, and stored in 70% ethanol at 4°C before paraffin embedding. Tissue sections were stained with hematoxylin and eosin. Images were taken using an Olympus Nanozoomer 2.0-HT System with NDP.scan 2.5 image software.

Western blotting

Adipose tissue and liver was homogenized by TissueLyzer beads in lysis buffer containing protease and phosphatase inhibitors (Cell Signaling, #9803; Roche, #04693124001 & 04906837001). Lysates were cleared of debris by centrifugation, and protein concentration was determined. 10% SDS-PAGE gels were used to run lysates and transferred to nitrocellulose membranes. Membranes were blocked in 5% milk and incubated overnight with the indicated primary antibodies. Proteins were visualized through use of HRP-conjugated secondary antibodies.

Microcomputed Tomography

Microcomputed tomography (μCT) was completed on tibias from 8 and 24-week-old mice. Buffered formalin (10%) fixed tibias were embedded in 2% agarose gel. The tibia, from the proximal epiphysis through the tibia-fibula junction, was scanned at 20-μm voxel resolution using a Scanco μCT 40 (Scanco Medical AG, Zurich, Switzerland). Measurements of both trabecular and cortical bone were made. For trabecular bone, 50 sections below the growth plate were contoured to exclude the cortical bone. For these trabecular regions, bone volume/tissue volume and bone mineral density (BMD) values were obtained. For cortical bone, the sections analyzed were 2 mm proximal to the tibia-fibula junction. Cortical bone area and tissue mineral density (TMD) were calculated from the contours of 20 sections per mouse. A threshold of 175 for trabecular bone and 260 for cortical bone (on a 0–1000 scale) was maintained.

Supplementary Material

Refer to Web version on PubMed Central for supplementary material.

Acknowledgments

The authors thank present and former members of the Mecham laboratory at Washington University and Dr. Francesco Ramirez at Mount Sinai School of Medicine for generously donating the *Fbn1*$^{+/-}$ (MgN) mouse line. This work was supported by National Institutes of Health grants: HL-053325 and HL-105314 to R.P.M, and PO1 AR049698 to L.Y.S. Additional support was received from the Shriners Hospitals for Children grants to L.Y.S., the American Diabetes Association grant 7-13-JF-16 to C.S.C., Washington University Nutrition and Obesity Research Center award P30-DK-056341 to C.S.C., and Washington University's Musculoskeletal Research Center award JIT2014_Craft_1 to C.S.C. Technical support was provided by the Mouse Phenotyping Core, the Adipocyte Biology and Molecular Nutrition Core of the Nutrition and Obesity Research Center (grant P30-DK-056341), the Morphology Core of the Digestive Disease Research Core Center (grant P30-DK-52574), and the Washington University Musculoskeletal Research Center structure and strength core (grant P30-AR-057235).

References

1. Alessi MC, Bastelica D, Morange P, Berthet B, Leduc I, Verdier M, Geel O, Juhan-Vague I. Plasminogen activator inhibitor 1, transforming growth factor-beta1, and BMI are closely associated in human adipose tissue during morbid obesity. Diabetes. 2000; 49:1374–1380. [PubMed: 10923640]
2. Carta L, Pereira L, Arteaga-Solis E, Lee-Arteaga SY, Lenart B, Starcher B, Merkel CA, Sukoyan M, Kerkis A, Hazeki N, Keene DR, Sakai LY, Ramirez F. Fibrillins 1 and 2 perform partially overlapping functions during aortic development. J Biol Chem. 2006; 281:8016–8023. [PubMed: 16407178]
3. Charbonneau NL, Carlson EJ, Tufa S, Sengle G, Manalo EC, Carlberg VM, Ramirez F, Keene DR, Sakai LY. In vivo studies of mutant fibrillin-1 microfibrils. J Biol Chem. 2010; 285:24943–24955. [PubMed: 20529844]
4. Corson GM, Charbonneau NL, Keene DR, Sakai LY. Differential expression of fibrillin-3 adds to microfibril variety in human and avian, but not rodent, connective tissues. Genomics. 2004; 83:461–472. [PubMed: 14962672]
5. Craft CS, Broekelmann TJ, Zou W, Chappel JC, Teitelbaum SL, Mecham RP. Oophorectomy-induced bone loss is attenuated in MAGP1-deficient mice. J Cell Biochem. 2012; 113:93–99. [PubMed: 21898536]
6. Craft CS, Pietka TA, Schappe T, Coleman T, Combs MD, Klein S, Abumrad NA, Mecham RP. The extracellular matrix protein MAGP1 supports thermogenesis and protects against obesity and diabetes through regulation of TGF-beta. Diabetes. 2014; 63:1920–1932. [PubMed: 24458361]

7. Craft CS, Zou W, Watkins M, Grimston S, Brodt MD, Broekelmann TJ, Weinbaum JS, Teitelbaum SL, Pierce RA, Civitelli R, Silva MJ, Mecham RP. Microfibril-associated glycoprotein-1, an extracellular matrix regulator of bone remodeling. J Biol Chem. 2010; 285:23858–23867. [PubMed: 20501659]
8. Finnis ML, Gibson MA. Microfibril-associated glycoprotein-1 (MAGP-1) binds to the pepsin-resistant domain of the alpha3(VI) chain of type VI collagen. J Biol Chem. 1997; 272:22817–22823. [PubMed: 9278443]
9. Franken R, den Hartog AW, de Waard V, Engele L, Radonic T, Lutter R, Timmermans J, Scholte AJ, van den Berg MP, Zwinderman AH, Groenink M, Mulder BJ. Circulating transforming growth factor-beta as a prognostic biomarker in Marfan syndrome. Int J Cardiol. 2013; 168:2441–2446. [PubMed: 23582687]
10. Habashi JP, Judge DP, Holm TM, Cohn RD, Loeys BL, Cooper TK, Myers L, Klein EC, Liu G, Calvi C, Podowski M, Neptune ER, Halushka MK, Bedja D, Gabrielson K, Rifkin DB, Carta L, Ramirez F, Huso DL, Dietz HC. Losartan, an AT1 antagonist, prevents aortic aneurysm in a mouse model of Marfan syndrome. Science. 2006; 312:117–121. [PubMed: 16601194]
11. Herder C, Zierer A, Koenig W, Roden M, Meisinger C, Thorand B. Transforming growth factor-beta1 and incident type 2 diabetes: results from the MONICA/KORA case-cohort study, 1984-2002. Diabetes care. 2009; 32:1921–1923. [PubMed: 19592635]
12. Isogai Z, Ono RN, Ushiro S, Keene DR, Chen Y, Mazzieri R, Charbonneau NL, Reinhardt DP, Rifkin DB, Sakai LY. Latent transforming growth factor beta-binding protein 1 interacts with fibrillin and is a microfibril-associated protein. J Biol Chem. 2003; 278:2750–2757. [PubMed: 12429738]
13. Judge DP, Biery NJ, Keene DR, Geubtner J, Myers L, Huso DL, Sakai LY, Dietz HC. Evidence for a critical contribution of haploinsufficiency in the complex pathogenesis of Marfan syndrome. J Clin Invest. 2004; 114:172–181. [PubMed: 15254584]
14. Judge DP, Dietz HC. Marfan's syndrome. Lancet. 2005; 366:1965–1976. [PubMed: 16325700]
15. Lin HM, Lee JH, Yadav H, Kamaraju AK, Liu E, Zhigang D, Vieira A, Kim SJ, Collins H, Matschinsky F, Harlan DM, Roberts AB, Rane SG. Transforming growth factor-beta/Smad3 signaling regulates insulin gene transcription and pancreatic islet beta-cell function. J Biol Chem. 2009; 284:12246–12257. [PubMed: 19265200]
16. Massam-Wu T, Chiu M, Choudhury R, Chaudhry SS, Baldwin AK, McGovern A, Baldock C, Shuttleworth CA, Kielty CM. Assembly of fibrillin microfibrils governs extracellular deposition of latent TGF beta. J Cell Sci. 2010; 123:3006–3018. [PubMed: 20699357]
17. Matt P, Schoenhoff F, Habashi J, Holm T, Van Erp C, Loch D, Carlson OD, Griswold BF, Fu Q, De Backer J, Loeys B, Huso DL, McDonnell NB, Van Eyk JE, Dietz HC, Gen TACC. Circulating transforming growth factor-beta in Marfan syndrome. Circulation. 2009; 120:526–532. [PubMed: 19635970]
18. Neptune ER, Frischmeyer PA, Arking DE, Myers L, Bunton TE, Gayraud B, Ramirez F, Sakai LY, Dietz HC. Dysregulation of TGF-beta activation contributes to pathogenesis in Marfan syndrome. Nat Genet. 2003; 33:407–411. [PubMed: 12598898]
19. Ng CM, Cheng A, Myers LA, Martinez-Murillo F, Jie C, Bedja D, Gabrielson KL, Hausladen JM, Mecham RP, Judge DP, Dietz HC. TGF-beta-dependent pathogenesis of mitral valve prolapse in a mouse model of Marfan syndrome. J Clin Invest. 2004; 114:1586–1592. [PubMed: 15546004]
20. Ono RN, Sengle G, Charbonneau NL, Carlberg V, Bachinger HP, Sasaki T, Lee-Arteaga S, Zilberberg L, Rifkin DB, Ramirez F, Chu ML, Sakai LY. Latent transforming growth factor beta-binding proteins and fibulins compete for fibrillin-1 and exhibit exquisite specificities in binding sites. J Biol Chem. 2009; 284:16872–16881. [PubMed: 19349279]
21. Ramirez F, Carta L, Lee-Arteaga S, Liu C, Nistala H, Smaldone S. Fibrillin-rich microfibrils - structural and instructive determinants of mammalian development and physiology. Connect Tissue Res. 2008; 49:1–6. [PubMed: 18293172]
22. Reber-Muller S, Spissinger T, Schuchert P, Spring J, Schmid V. An extracellular matrix protein of jellyfish homologous to mammalian fibrillins forms different fibrils depending on the life stage of the animal. Dev Biol. 1995; 169:662–672. [PubMed: 7781906]

23. Sakai LY, Keene DR, Engvall E. Fibrillin, a new 350-kD glycoprotein, is a component of extracellular microfibrils. J Cell Biol. 1986; 103:2499–2509. [PubMed: 3536967]
24. Smaldone S, Ramirez F. Fibrillin microfibrils in bone physiology. Matrix Biol. 2015
25. Srivastava M, Begovic E, Chapman J, Putnam NH, Hellsten U, Kawashima T, Kuo A, Mitros T, Salamov A, Carpenter ML, Signorovitch AY, Moreno MA, Kamm K, Grimwood J, Schmutz J, Shapiro H, Grigoriev IV, Buss LW, Schierwater B, Dellaporta SL, Rokhsar DS. The Trichoplax genome and the nature of placozoans. Nature. 2008; 454:955–960. [PubMed: 18719581]
26. Tan CK, Leuenberger N, Tan MJ, Yan YW, Chen Y, Kambadur R, Wahli W, Tan NS. Smad3 deficiency in mice protects against insulin resistance and obesity induced by a high-fat diet. Diabetes. 2011; 60:464–476. [PubMed: 21270259]
27. Tiano JP, Springer DA, Rane SG. SMAD3 negatively regulates serum irisin and skeletal muscle FNDC5 and peroxisome proliferator-activated receptor gamma coactivator 1-alpha (PGC-1alpha) during exercise. J Biol Chem. 2015; 290:7671–7684. [PubMed: 25648888]
28. Weinbaum JS, Broekelmann TJ, Pierce RA, Werneck CC, Segade F, Craft CS, Knutsen RH, Mecham RP. Deficiency in microfibril-associated glycoprotein-1 leads to complex phenotypes in multiple organ systems. J Biol Chem. 2008; 283:25533–25543. [PubMed: 18625713]
29. Yadav H, Quijano C, Kamaraju AK, Gavrilova O, Malek R, Chen W, Zerfas P, Zhigang D, Wright EC, Stuelten C, Sun P, Lonning S, Skarulis M, Sumner AE, Finkel T, Rane SG. Protection from obesity and diabetes by blockade of TGF-beta/Smad3 signaling. Cell Metab. 2011; 14:67–79. [PubMed: 21723505]
30. Yan J, Zhang H, Yin Y, Li J, Tang Y, Purkayastha S, Li L, Cai D. Obesity- and aging-induced excess of central transforming growth factor-beta potentiates diabetic development via an RNA stress response. Nat Med. 2014; 20:1001–1008. [PubMed: 25086906]
31. Zhang H, Apfelroth SD, Hu W, Davis EC, Sanguineti C, Bonadio J, Mecham RP, Ramirez F. Structure and expression of fibrillin-2, a novel microfibrillar component preferentially located in elastic matrices. J Cell Biol. 1994; 124:855–863. [PubMed: 8120105]
32. Zhang H, Hu W, Ramirez F. Developmental expression of fibrillin genes suggests heterogeneity of extracellular microfibrils. J Cell Biol. 1995; 129:1165–1176. [PubMed: 7744963]

Abbreviations

Fbn1	fibrillin-1
MFS	Marfan syndrome
TGFβ	transforming growth factor-beta
MAGP	microfibril-associated glycoprotein
Fbn2	fibrillin-2
ECM	extracellular matrix
LTBP	latent TGFβ binding protein
BAT	brown adipose tissue
epWAT	epididymal white adipose tissue
scWAT	subcutaneous white adipose tissue
μCT	microcomputed tomography

Highlights

- Fibrillin-1 mutation in mice does not reduce fat or muscle mass, as observed in humans
- Fibrillin-1 mutation increases TGF-β activity in bone, but not in adipose tissue
- Fibrillin-1 and MAGP1 similarly regulate bone remodeling, but only MAGP1 alters adiposity

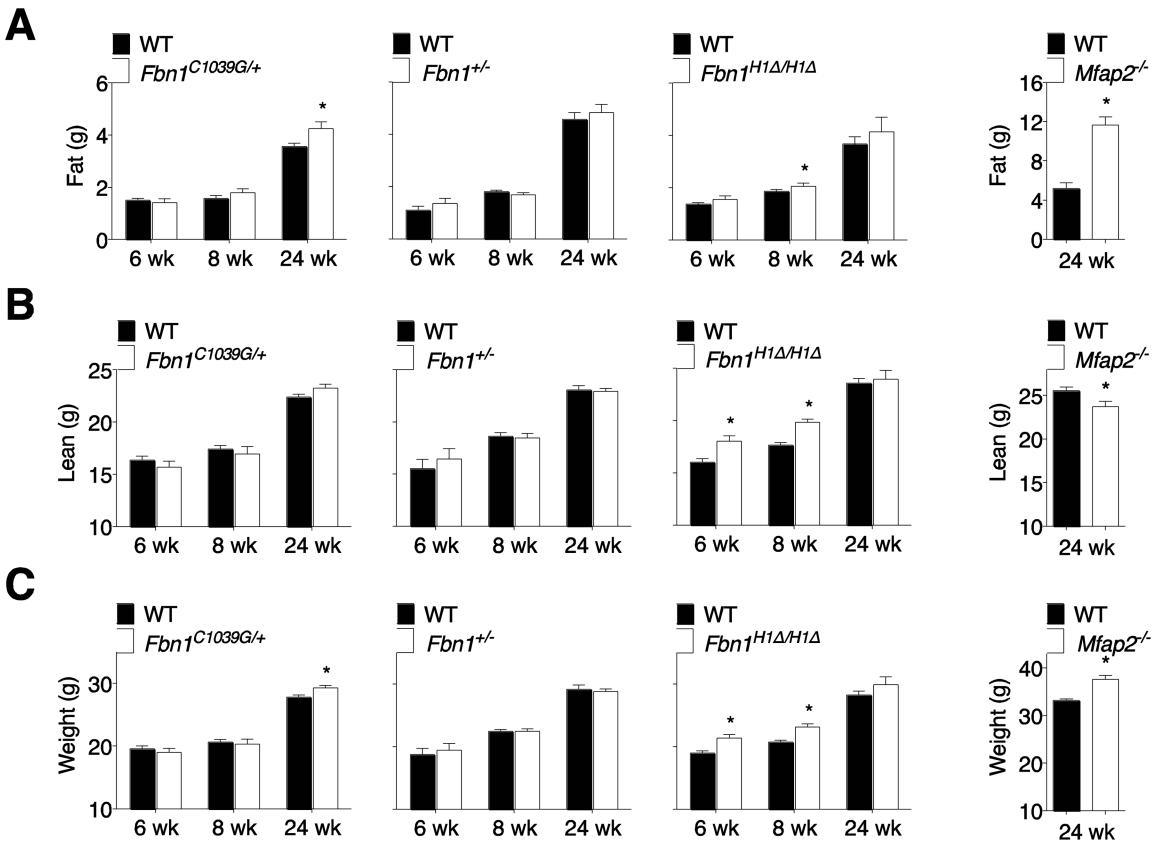

Figure 1.

Fibrillin-1 mutation in mice has little effect on fat and muscle. A-C: Longitudinal study of whole-body fat and lean content was determined by EchoMRI at 6 weeks (A), 8 weeks (B), and 24-weeks of age (C). Mean ± SEM; Mfn: 6 wk n = 13,8; 8 wk n = 10,8; 24 wk n = 10,8. MgN: 6 wk n = 10,8; 8 wk n = 13,11; 24 wk n = 21,20. H1Δ: 6 wk n = 8,10; 8 wk n =25,18; 24 wk n =10,10. MAGP1: 24 wk n = 6,8. Student *t* test was used for single comparisons (P* ≤0.05).

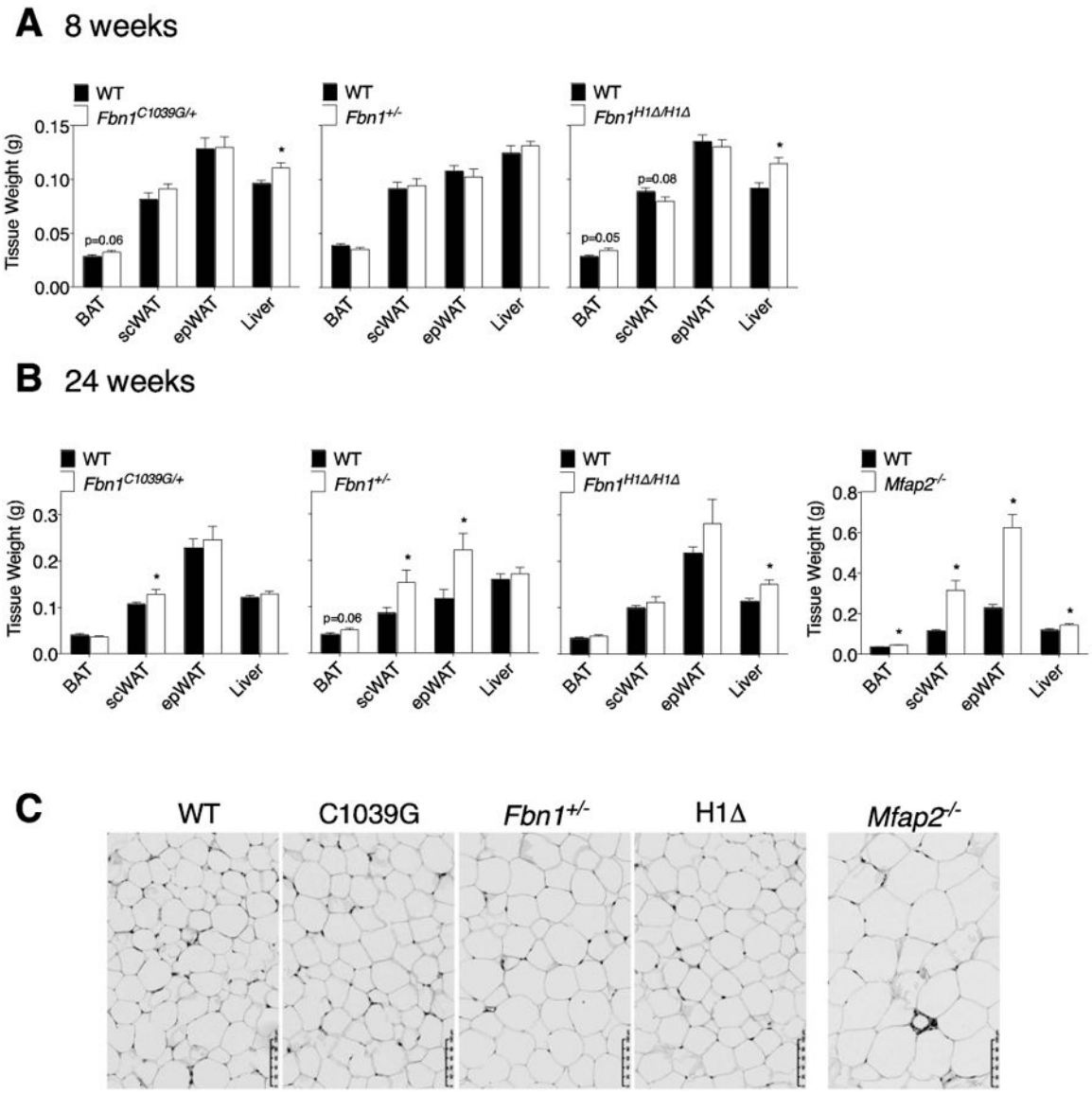

Figure 2.

Metabolic tissue masses from fibrillin-1 and MAGP1 mutant mice A-B: Tissue were harvested at 8 weeks (A) and 24 weeks of age (B) (mean ± SEM; Mfn: 8 wk n =11,10; 24 wk n = 15,11; MgN: 8 wk n =10,9; 24 wk n = 11,13; H1Δ: 8 wk n = 16,15; 24 wk n = 13,8; MAGP1: 24 wk n = 6,8). C: Representative images of hematoxylin-eosin stained epWAT from 24 week WT, fibrillin-1 mutant mice, and *Mfap2*$^{-/-}$ mice (20×, scale bar 100 μm). Student *t* test was used for single comparisons (P* ≤0.05).

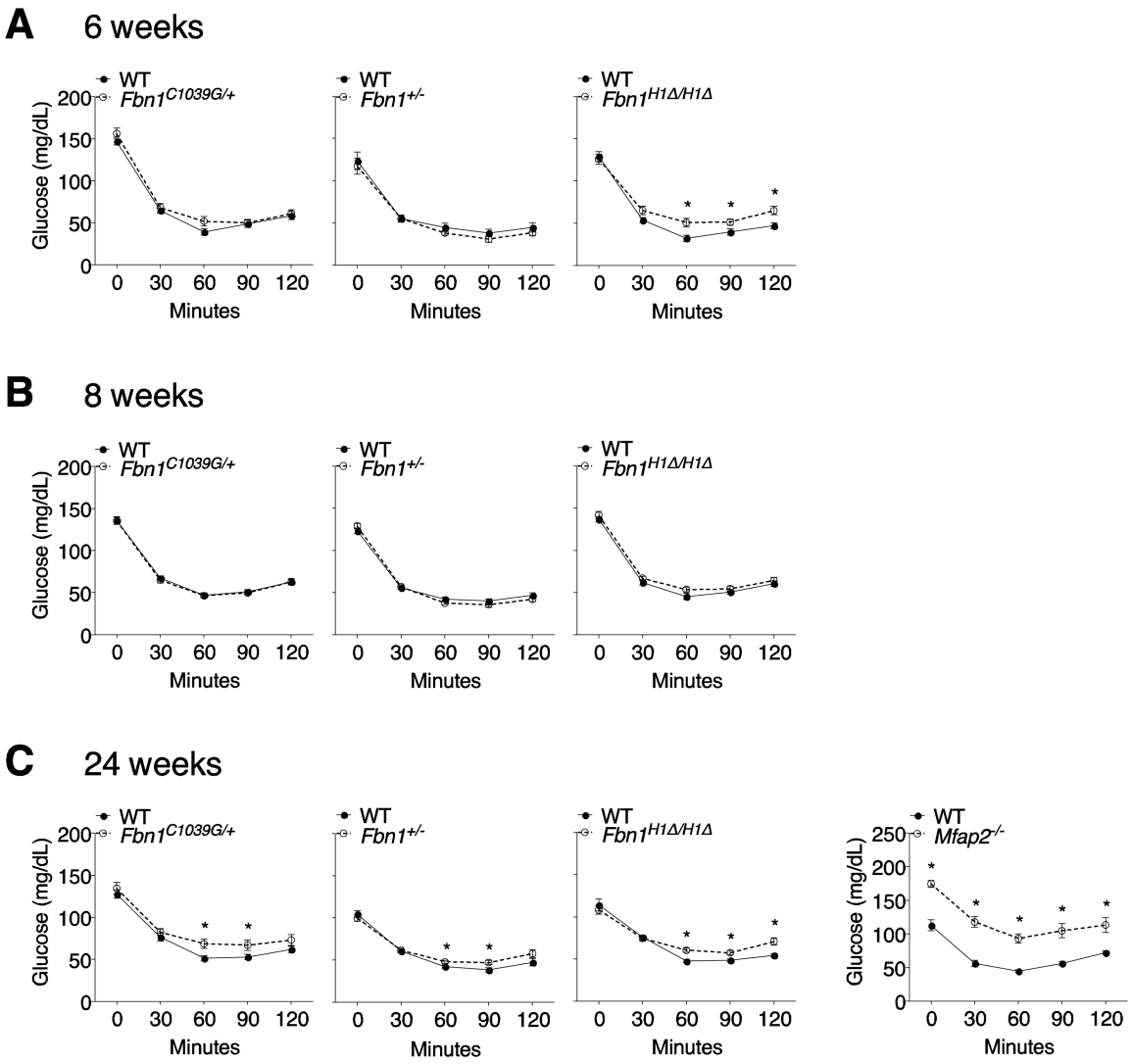

Figure 3.

Insulin sensitivity is reduced in adult fibrillin-1 mutant mice. A-C: ITT results following a 6-hour fast and 0.75 units/kg insulin injection in 6-,8-,24- week fibrillin-1 mutant mice. Mean ± SEM; Mfn: 6 wk n = 17,9; 8 wk n = 23,17; 24 wk n = 17,12. MgN: 6 wk n = 11,9; 8 wk n = 31,23; 24 wk n = 24,24. H1Δ: 6 wk n =7,10; 8 wk n =28,25; 24 wk n =12,13. MAGP1: 24 wk n = 5,8. Student *t* test was used for single comparisons (P* ≤0.05).

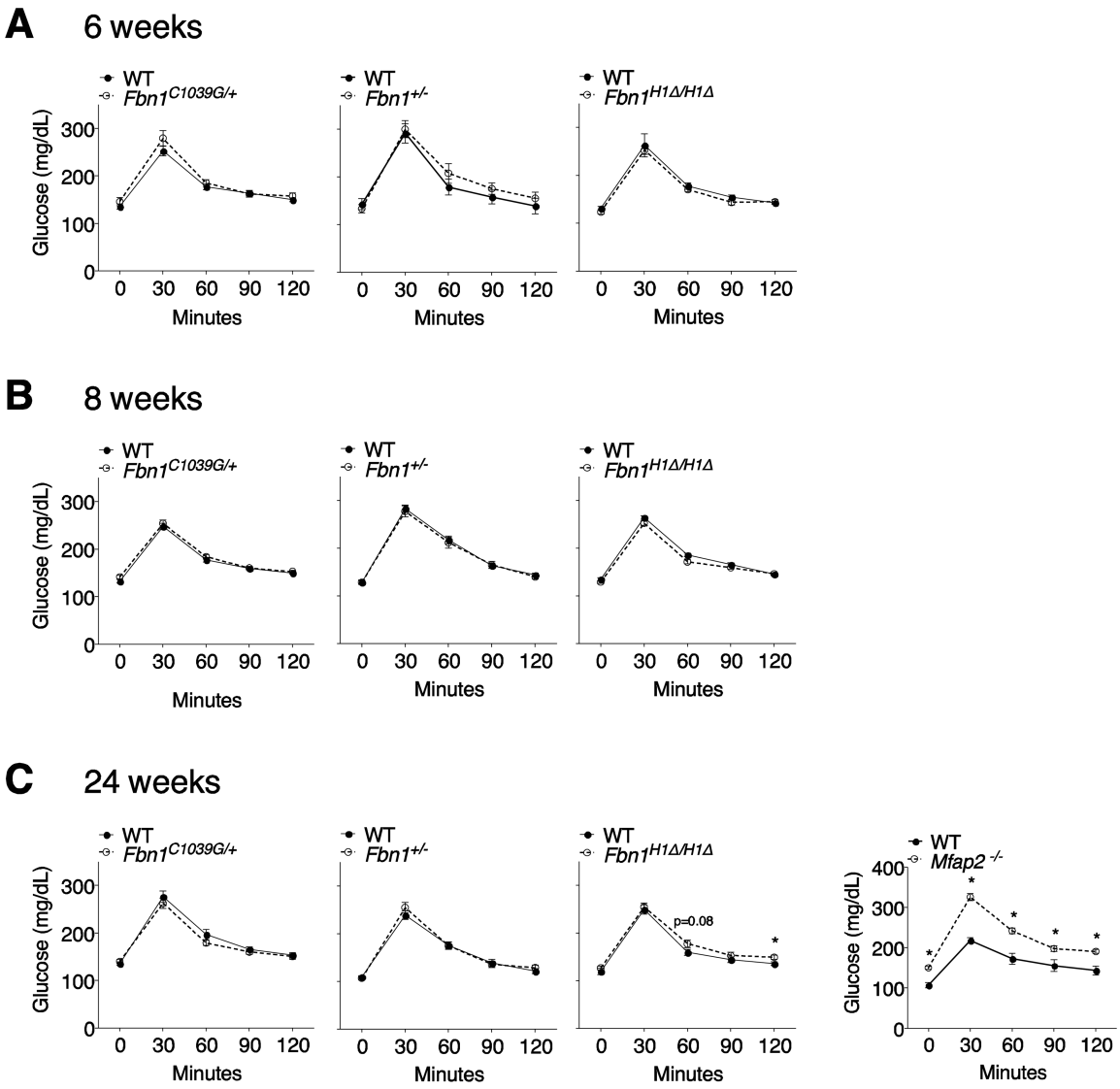

Figure 4.

Glucose tolerance is normal at all ages in Fibrillin-1 mutant mice. A-C: GTT results following a 6-hour fast and 1g/kg dextrose injection in 6-,8-,24- week old fibrillin-1 mutant mice. Mean ± SEM; Mfn: 6 wk n = 14,9; 8 wk n = 21,18; 24 wk n = 16,12. MgN: 6 wk n = 8,9; 8 wk n = 30,26; 24 wk n = 24,27. H1Δ: 6 wk n =7,10; 8 wk n =28,28; 24 wk n =13,13. MAGP1: 24 wk n = 5,8. Student *t* test was used for single comparisons (P* ≤0.05).

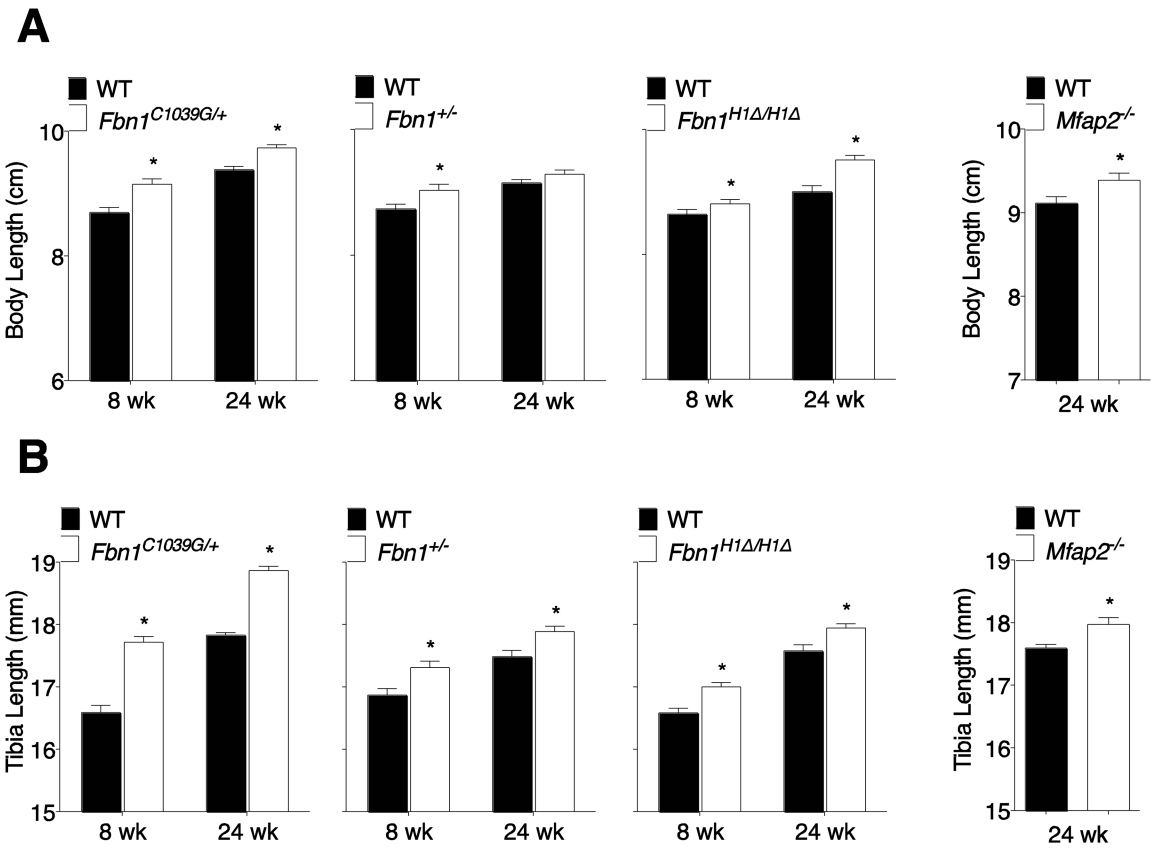

Figure 5.

Fibrillin-1 and MAGP1 mutant mice display long bone overgrowth. A: Body length measured from nose tip to tail base at 8 and 24 weeks. Mean ± SEM; Mfn: 8 wk n =13,10; 24 wk n = 17,12; MgN: 8 wk n =11,9; 24 wk n = 12,13; H1Δ: 8 wk n = 18,16; 24 wk n = 13,8; MAGP1: 24 wk n = 6,8. B: Tibia length measured by digital calipers after all soft tissue had been removed at 8 to 24 weeks. Mean ± SEM; Mfn: 8 wk n =13,10; 24 wk n = 17,12; MgN: 8 wk n =11,9; 24 wk n = 12,13; H1Δ: 8 wk n = 18,16; 24 wk n = 13,8; MAGP1: 24 wk n = 6,8. Student *t* test was used for single comparisons (P* ≤0.05).

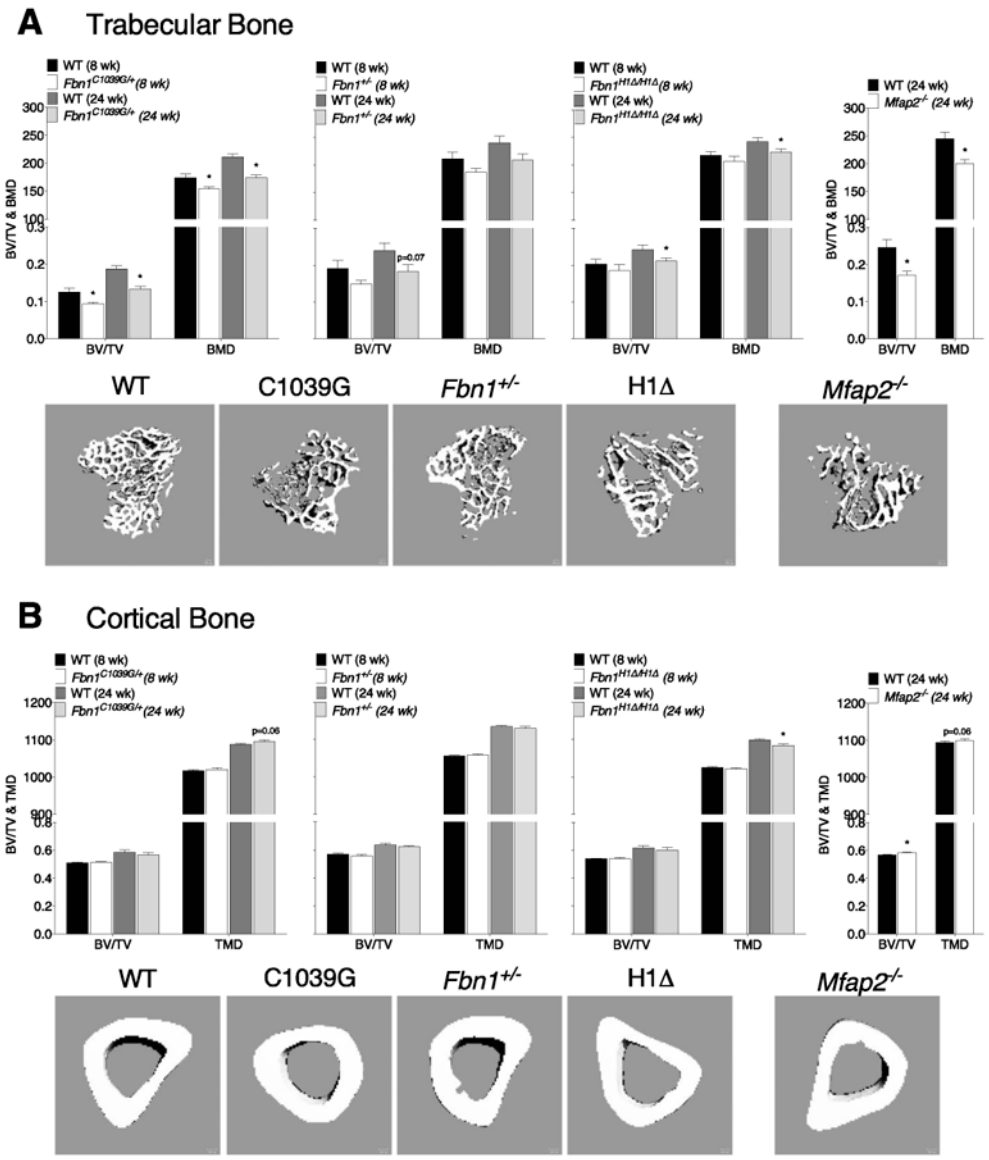

Figure 6.

Fibrillin-1 and MAGP1 mutant mice have reduced bone mass. A-B: Tibias were harvested from 8-and 24-week-old mice. Micro-computed tomography was used to determine the ratio of bone volume to total volume (BV/TV) and bone mineral density (BMD). For trabecular bone, the first 50 – 20um slices distal to the growth plate were analyzed. For cortical bone, BV/TV and total mineral density (TMD) was determined by contouring 20 – 20μm slices. Mean ± SEM; Mfn: 8 wk n =10,7; 24 wk n = 17,12; MgN: 8 wk n =9,7; 24 wk n = 7,8; H1Δ: 8 wk n = 16,14; 24 wk n = 13,13; MAGP1: 24 wk n = 6,8. Student *t* test was used for single comparisons (P* ≤0.05).

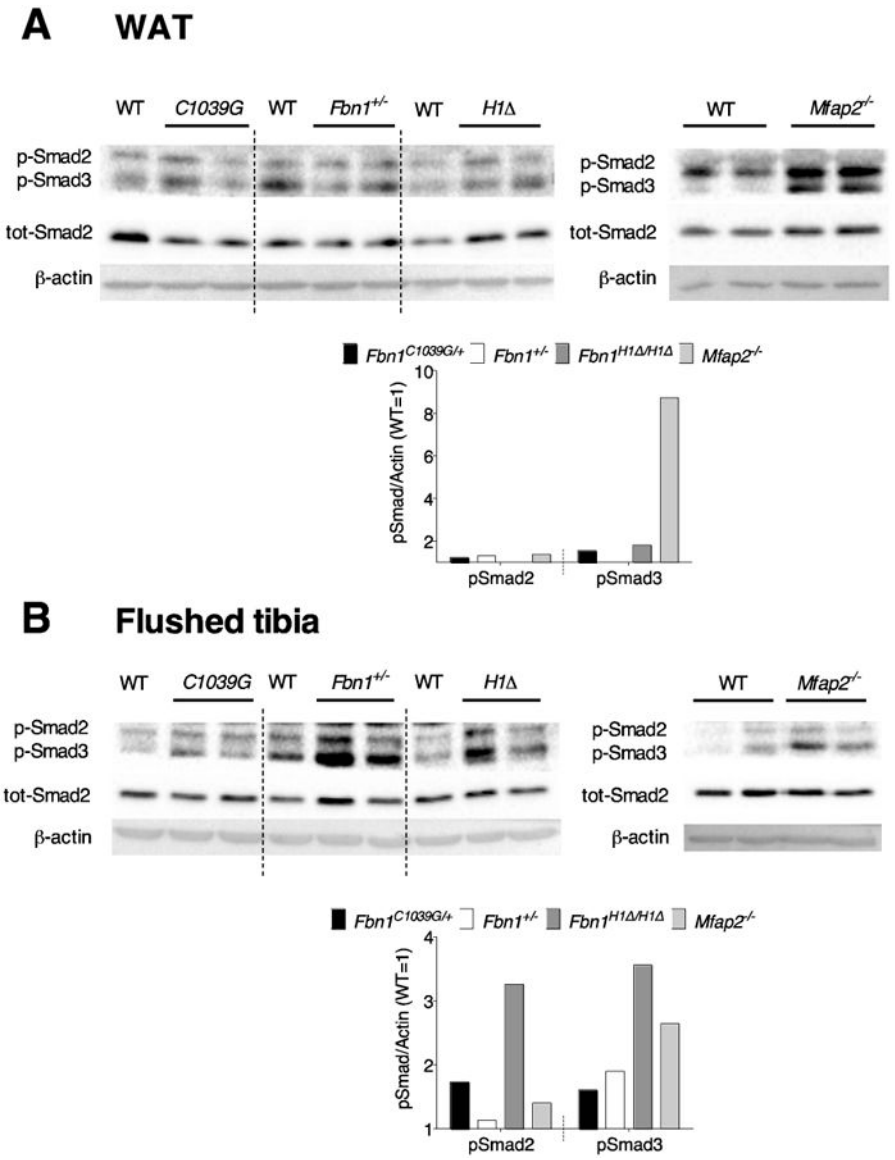

Figure 7.

Tissue specific regulation of TGFβ by fibrillin-1. A-B: Immunoblot of (A) epWAT and (B) flushed tibia lysate using antibodies to phosphorylated Smad-2/-3 (p-Smad2/3), total Smad2 (tsmad2), and β-actin. Bar graph values represent the ratio of phosphorylated protein to loading control. The ratio was calculated by averaging the band intensity of replicate wells.

Matrix Biol. Author manuscript; available in PMC 2017 September 01.

Table 1

Phenotypes of microfibril mutant mice

Mouse Model (Reference)	Mutation	Skeletal	Metabolic	Cardiovascular	Pulmonary	Skin	Lifespan
***Mfap2*$^{-/-}$ (MAGP1)** (*i*)	Null allele	***Osteopenia, long bone overgrowth***	Reduced energy expenditure, ***excess adiposity, impaired glucose metabolism***	Normal	Normal, protection from emphysema		Normal
***Mfap5*$^{-/-}$ (MAGP2)** (*ii*)	Null allele	Normal		TAA in humans	Normal		Normal
MAGP1;MAGP2-DKO (*iii*)	Null allele	Osteopenia		Aortic dilation			
***Fbn1*$^{+/-}$ (MgN)** *iv*	Null allele	***Reduced bone mass, slight long bone overgrowth***	***Slightly elevated fat mass and reduced insulin sensitivity in aged animals***				Normal
Fbn1$^{mgR/mgR}$ (*v, vi, vii*)	Low expression of wild-type *Fbn1*	Osteopenia, kyphosis, long bone overgrowth (10%)		Thoracic aortic aneurysm, dilated cardiomyopathy, normal BP	airspace enlargement, diaphragmatic hernia		3-4 months
Fbn1$^{C1039G/+}$ (*viii*)	missense mutation substituting glycine for cysteine	Kyphosis, rib overgrowth ***Reduced bone mass, long bone overgrowth***	***Slightly elevated fat mass and reduced insulin sensitivity in aged animals***	Thoracic aortic aneurysms, mitral valve prolapse	airspace enlargement		Normal
***Fbn1*$^{mg\Delta/mg\Delta}$** (*ix*)	deletion of exons 19-24	Normal		Thoracic aortic aneurysms	airspace enlargement, pulmonary hemorrhage		14 days in homozygous
mgΔ^{loxPneo} (*x*)	deletion of exons 19-24 and *neoR* flanked by lox-P sequences	Kyphosis		Aortic medial thickening, aortic rupture			14 days in homozygous (background dependent)
***Fbn1*$^{TSK1/+}$** (*xi*)	large in-frame duplication	Long bone overgrowth, abnormal cartilage		cardiac hypertrophy	airspace enlargement	Tight skin, thickened dermal layer	Embryonic lethality in homozygous (E7-8)
***Fbn1*$^{GT-8/+}$** (*xii*)	truncation, tagged with eGFP		Abnormal skeletal muscle	fragmented elastic lamellae		Fragmented elastic	Between P9-p18 in homozygous
***Fbn1*$^{H1\Delta/H1\Delta}$** (*xiii*)	deletion of exon 7	Normal skeletal development, ***Reduced bone mass, slight long bone overgrowth***	***Slightly elevated fat mass and reduced insulin sensitivity in aged animals***	normal	normal	Normal	Normal

Mouse Model (Reference)	Mutation	Skeletal	Metabolic	Cardiovascular	Pulmonary	Skin	Lifespan
Fbn1$^{wm\Delta/wm\Delta}$ (*xiv*)	deletion of exons 9-11	Brachydactylic, reduced bone growth (normal after 5 mo)		normal		Thick skin	Normal?
Fbn2$^{-/-}$ (*xv,xvi*)	Null allele	Fused Phalanges (syndactyly), reduced limb length	Postnatal growth retardation, decreased body sixe, abnormal skeletal muscle				Normal
Fbn2$^{-/-}$ **(129 background)** (*xvii*)	null allele with 129 background	Forelimb contractures	Reduced muscle mass, abnormal muscle histology, delayed muscle differentiation, white fat in forelimbs (redcued by BMP7)		Respiratory failure on B6		

[i] Weinbaum, JBC, 2008; Craft, JBC, 2010; Craft, J Cell Biochem, 2012; Craft, 2014, Mecham, MatBio, 2015

[ii] Combs, JBC, 2013; Barbier, Am J Hum Genet, 2014

[iii] Combs, JBC, 2013

[iv] Carta, JBC, 206

[v] Pereira, PNAS, 1999; Nistala, HumMolGen, 2010

[vi] Cook, JCI, 2014

[vii] Marque, ATVB, 2001

[viii] Judge, JCI, 2004; Ng et al, JCI, 2004

[ix] Pereira, Nat Gen, 1997

[x] Lima, PlosOne, 2010

[xi] Green, Am J Pathol., 1976; Menton, JID, 1980

[xii] Charbonneau, JBC, 2010

[xiii] Charbonneau, JBC, 2010

[xiv] Sengle PlosGenet, 2012

[xv] Arteaga-Solis, J Cell Biol, 2001; Chaudhry, HumMolGen, 2001

[xvi] Miller, PlosOne, 2010

[xvii] Sengle, PlosGenet, 2015